Slow γ photon with a doublet structure: Time delay via a transition from destructive to constructive interference of collectively scattered radiation with the incoming photon

R. N. Shakhmuratov,[1] F. Vagizov,[2,3] J. Odeurs,[4] and O. Kocharovskaya[3]
[1]*Kazan Physical-Technical Institute, Russian Academy of Sciences, 10/7 Sibirsky Trakt, Kazan 420029, Russia*
[2]*Kazan State University, 18 Kremlyovskaya Street, Kazan 420008, Russia*
[3]*Department of Physics and Institute for Quantum Studies, TAMU, College Station, Texas 77843-4242, USA*
[4]*Instituut voor Kern- en Stralingsfysica, Katholieke Universiteit Leuven, Celestijnenlaan 200 D, B-3001 Leuven, Belgium*
(Received 8 July 2009; published 2 December 2009)

Single γ photon propagation in a dense absorptive medium with two widely spaced resonances is experimentally studied. After an initial fast decay, a revival of the photon amplitude in the form of a bump, exceeding the probability amplitude of the incident photon, is observed. The irradiation time of this bump delays approximately by the lifetime of the excited nuclei in the absorber. This effect is explained by the interference of the incoming radiation with the collectively scattered radiation, the phase of which is modulated with the frequency of the doublet splitting. Initially, the destructive interference changes to a constructive one, distinguishing the storage and retrieval stages of the photon propagation in a dense medium, i.e., the collective absorption and collective re-emission processes.

DOI: 10.1103/PhysRevA.80.063805 PACS number(s): 42.50.Gy

I. INTRODUCTION

The single-photon interaction with a resonant medium is of importance from a fundamental point of view and from applications in quantum cryptography and quantum computing (see, for example, [1] and references therein). It is remarkable that since its discovery, Mössbauer spectroscopy has worked with sources emitting single photons. Even the invention of synchrotron radiation sources of extremely high brilliance did not change the situation in Mössbauer spectroscopy because the spectrum of synchrotron radiation spreads from visible light to hard x-rays with the upper limit extending up to 100 keV, while a typical value for the natural nuclear resonance width, for example, for ^{57}Fe, is $\approx 2 \times 10^{-8}$ eV (see, for example, Ref. [2]). Many interesting experiments with single-photon sources and synchrotron radiation have been performed demonstrating the collective excitation of nuclei incorporated into a solid. Because of the small resonant cross section of the nucleus, thick resonant absorbers have been studied. A γ photon incident on an ensemble of nuclei can interact resonantly with each nucleus. Meanwhile, the energy of the one photon is only sufficient to excite a single nucleus in the ensemble. However, the observation of Bragg diffraction in a perfect crystal demonstrates that we have a collective nature of scattering of a single γ photon by the ensemble, instead of scattering only by a single nucleus [2]. This happens because, in the scattered radiation, we cannot distinguish which nucleus has scattered the photon. By one of the rules of quantum mechanics, we must sum all probability amplitudes of the photon evolution in the absorber, which takes into account scattering in all nuclei including the multiple scattering events. All these "quantum trajectories" of the photon in the ensemble of nuclei give the complete probability amplitude of the photon at the output of the absorber. The collective excitation of an ensemble of nuclei by a γ photon was named by Trammell [3], and Kagan and Afanas'ev [4] the delocalized nuclear excitation or "nuclear exciton." The nuclear exciton has become a central concept of the theory of nuclear resonant scattering. It was shown that the nuclear ensemble behaves like a macroscopic resonator with properties qualitatively different from those of an individual nucleus [2].

Controllable delay, storage, and retrieval of a single photon are important in quantum communication and information processing where single photons have been proposed to use as "flying quantum bits," connecting spatially separated nodes in a quantum network [5]. Excellent buffers for data synchronization can be constructed with the help of electromagnetically induced transparency (EIT) [6,7]. Recently, it was clearly demonstrated that electromagnetic pulses are delayed and can even be "stopped" in an optically dense medium with a narrow transparency window in the absorption spectrum controlled by an auxiliary excitation field [8,9]. The storage and retrieval of photon pairs with EIT even allowed to essentially increase their coherence time [10]. An appreciable delay of electromagnetic pulses can be realized also without an auxiliary excitation of a resonant medium. It was observed in a dense medium with two widely spaced absorption resonances [11–14]. The slowing down of the group velocity of the pulse is due to normal dispersion in the middle of the doublet structure. It has been explained by the energy storage of the pulse in the excited atomic states [15]. The pulse is appreciably delayed and its shape is not corrupted if the pulse duration is shorter than the lifetime of the atomic excited state and its bandwidth is smaller than the doublet splitting. Single-photon propagation under these conditions has been analyzed in Ref. [15].

In this paper, we study the propagation of a single γ photon in a dense absorptive medium with a doublet structure. The available radiation source and the nuclei in the absorber have the same linewidth in our experiment, and hence, the condition [15] of the long lifetime of the excited nuclei in the absorber compared with the coherence time of a source photon is not fulfilled. Therefore, we cannot expect a delay of a

photon wave packet exceeding appreciably its coherence time. However, in an absorber with moderate thickness, we have observed a photon delay approximately equal to the lifetime of the excited nuclei. Interference of the photon quantum paths has been considered. We have shown that the delay is caused by destructive interference of these paths due to quantum beats.

The paper is organized as follows. In Sec. II, we present the definition of a single-photon field. In Sec. III, we represent the formalism of the description of multiple scattering of a photon in an absorber with a single resonance. In Sec. IV, we consider multiple scattering of a photon in an absorber with two resonances. In Sec. V, we derive the response function of a thick absorber with a doublet structure. In Sec. VI, we analyze our results from the view point of the group velocity concept. In Secs. VII and VIII, experimental results and their discussion are presented.

II. RADIATION FIELD OF THE SOURCE NUCLEUS

In the absence of hyperfine splitting of the nuclear levels, the source nucleus in the excited state emits a spherically symmetric wave packet. The radiation state of this wave packet, for long times,

$$|b\rangle = \sum_{\mathbf{k}} g_{\mathbf{k}} \frac{\exp(-i\mathbf{k}\cdot\mathbf{r}_0)}{\nu_k + i\gamma} |1_{\mathbf{k}}, \{0_{\mathbf{q}}\}\rangle, \tag{1}$$

consists of many single-photon Fock states $|1_{\mathbf{k}}, \{0_{\mathbf{q}}\}\rangle$, which contain one photon in the mode ω_k with wave vector $\mathbf{k}$ and other modes with $\mathbf{q} \neq \mathbf{k}$, denoted by $\{0_{\mathbf{q}}\}$, are empty. The radiation state (1) is normalized such that in total it contains only one photon. Here, $\mathbf{r}_0$ is the location of the emitting nucleus, $\nu_k = \omega_k - \omega_0$ is the frequency difference of the $\mathbf{k}$ mode and the resonant transition from the excited state e to the ground state g, and 2γ is the decay rate of the excited state e (radiative and nonradiative if present). The coupling parameter of the radiation with the source is $g_{\mathbf{k}}$. Defining the electric field operator

$$E^{(+)}(\mathbf{r},t) = \sum_{\mathbf{k}} \hat{\boldsymbol{\epsilon}}_{\mathbf{k}} \mathcal{E}_{\mathbf{k}} a_{\mathbf{k}} e^{-i\nu_k t + i\mathbf{k}\cdot\mathbf{r}}, \tag{2}$$

which contains only the annihilation operators $a_{\mathbf{k}}$, the unit polarization vector $\hat{\boldsymbol{\epsilon}}_{\mathbf{k}}$, and the normalized amplitude $\mathcal{E}_k$ of the mode $\mathbf{k}$, we can calculate the single-photon field

$$b(t) = \langle 0|E^{(+)}(\mathbf{r},t)|b\rangle. \tag{3}$$

Here, for simplicity, we omit the vector notation for the single-photon field. Performing the sum over the wave vector $\mathbf{k}$ in the expression for the single-photon field, one obtains [16]

$$b(t) = \frac{\mathcal{E}_0}{d} \Theta(t - d/c) e^{-(i\omega_0 + \gamma)(t - d/c)}, \tag{4}$$

where $d = |\mathbf{r} - \mathbf{r}_0|$ is the distance from the source, $\mathcal{E}_0$ is a normalized amplitude and $\Theta(t)$ is the Heaviside step function, assuring causality. This wave packet has a sharply rising leading edge at $t = d/c$ and an exponentially decaying tail. The former is defined by the time $t_0 = 0$ at which the source is formed in the excited state and the latter specifies the coherence time or the mean correlation time of the photon $\tau_{\mathrm{ph}} = 1/\gamma$. Such a time dependence of the single-photon field has been detected, using radiation of a single nucleus in time delayed-coincidence measurements of γ photons emitted in a nuclear cascade [17–22].

Lynch *et al.* [17] empirically introduced a similar expression for the source photon within a classical theory of γ photon propagation in a dense resonant absorber. A single-photon radiation field is presented as a damped electric field $b(t) = b_0(t)\exp(-i\omega_0 t)$, where the distance d from the source is neglected and the amplitude of the field at the input of the absorber,

$$b_0(t) = \Theta(t) e^{-\gamma t}, \tag{5}$$

is normalized to unity. Later, Harris [23] derived quantum mechanically the same expression confirming the empirical approach of Lynch. In the theory of Harris, the radiative and nonradiative channels of the decay of the excited nucleus via conversion electron have been taken into account.

If we adopt the Fourier transform of the form

$$F(\nu) = \int_{-\infty}^{+\infty} f(t) e^{i\nu t} dt, \tag{6}$$

the Fourier transform of the radiation field amplitude (5) is

$$B_0(\nu) = \frac{i}{\nu + i\gamma}. \tag{7}$$

III. COHERENT SCATTERING OF A PHOTON IN A RESONANT ABSORBER

In this section, we briefly outline the method of description of the photon propagation in a medium where the resonant nuclei are incorporated randomly and do not form a regular structure. Hence, no Bragg scattering is present. An incident photon, represented by a plane wave at the input of absorber, is scattered coherently only in the forward direction by all nuclei, and propagates inside (see, for example, Ref. [2]). There is no coherent scattering in other directions because of destructive interference. Incoherent scattering in other directions may take place, but its probability is much smaller than the probability of coherent scattering in the forward direction. The classical [17] and quantum mechanical [23] theories give the following expression for the probability amplitude of a photon at the output of the resonant absorber:

$$b(z,t) = \frac{1}{2\pi} \int_{-\infty}^{+\infty} B_0(\nu) \exp[-i\nu(t - z/c) - A(\nu)z] d\nu, \tag{8}$$

where z is the physical thickness of the absorber and $A(\nu)$ is the transmission function, which is defined by a complex dielectric constant or which can be calculated from the response of a single nucleus to the incident radiation. If the nuclei in the absorber have a single absorption line tuned in resonance with the source photon, the transmission function can then be expressed as follows:

$$A(\nu) = \frac{i\alpha_0}{\nu + i\gamma}, \tag{9}$$

where $2\alpha_0/\gamma$ is the absorption coefficient α_B, i.e., Beer's law coefficient applicable to a monochromatic radiation tuned in resonance.

For a single-photon radiation field (7), the integral in Eq. (8) has been calculated in Refs. [17,24]. The result is

$$b(z,t) = e^{-\gamma t} J_0(\sqrt{2T\gamma t})\Theta(t), \tag{10}$$

where $T=2\alpha_0 z/\gamma=\alpha_B z$ is the effective thickness of the absorber and z/c is neglected since it is small. The integral is calculated with the help of the generating function for the Bessel function. Below, we calculate this integral by applying a different technique to show the role of multiple scattering. Our approach is important for the explanation of photon scattering in the absorber with a doublet structure.

Expanding $\exp[-A(\nu)z]$ in a power series in Eq. (8), we can express the transmitted radiation as a sum

$$b(z,t) = \sum_{n=0}^{\infty} b_n(t), \tag{11}$$

where

$$b_n(t) = \frac{(-z)^n}{2\pi n!} \int_{-\infty}^{+\infty} e^{-i\nu t} B_0(\nu) A^n(\nu) d\nu. \tag{12}$$

can be interpreted as radiation scattered n times. For example, the term with $n=0$ corresponds to the radiation passed through the absorber without scattering, the term with $n=1$ corresponds to the radiation produced by all nuclei scattering only one time each, the term with $n=2$ corresponds to the radiation produced by nuclei undergoing first a single scattering and then one rescattering, i.e., it is radiation produced by all nuclei participating in one rescattering event. Generally, n corresponds to radiation formed by $(n-1)$-times rescattering events (multiple scattering) where all nuclei in the absorber participate. Calculating the integral in Eq. (12), we obtain

$$b_n(t) = e^{-\gamma t}\Theta(t)\frac{(-T\gamma t/2)^n}{(n!)^2}. \tag{13}$$

The sum (11) of the multiple scattering components of the radiation field gives the expansion of the Bessel function $J_0(\sqrt{2T\gamma t})$ in a power series, multiplied by $\exp(-\gamma t)\Theta(t)$. Here, it is important to notice that each scattering event changes the phase of the scattered field by π. For example, single scattering produces a field that is in antiphase with the incoming radiation. This point is discussed in every detail, for example, in Refs. [25,26].

IV. COHERENT SCATTERING IN A DOUBLET STRUCTURE

We consider the excitation scheme discussed in Ref. [15], see Fig. 1. The nuclei in the absorber experience a quadrupole splitting 2Δ of the excited state, forming a doublet structure of two closely spaced excited states e_1 and e_2. The carrier frequency of the source photon ω_0 is tuned to the middle ω_m of this doublet structure. We assume that the spectral width of the photon $2\gamma=2/\tau_{\rm ph}$ is smaller than the splitting 2Δ. For simplicity, we consider an equal strength of the interaction of a single photon for both transitions: $g\rightarrow e_1$ and $g\rightarrow e_2$. Then, the transmission function of the absorber with the doublet structure is [15]

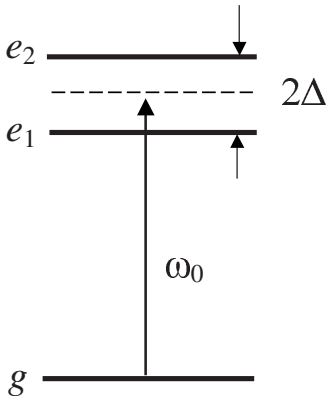

FIG. 1. The excitation scheme of a nucleus in the absorber by a single photon with frequency ω_0, which is tuned to the middle of the two excited states separated by an energy $2\hbar\Delta$.

$$A(\nu) = \frac{i\alpha_0/2}{\nu + \Delta + i\gamma} + \frac{i\alpha_0/2}{\nu - \Delta + i\gamma}. \tag{14}$$

If the transition probabilities are not equal, then the photon carrier frequency ω_0 should be detuned from the middle of the doublet ω_m to the frequency $\omega_m+\omega_n$, which corresponds to peak transmission. The detuning is $\omega_n \approx (\alpha_1^{1/3}-\alpha_2^{1/3})\Delta/(\alpha_1^{1/3}+\alpha_2^{1/3})$, where α_1 and α_2 account for the transition probabilities $g\rightarrow e_1$ and $g\rightarrow e_2$, respectively. However, for example, in the experiment described in Ref. [14], where $\alpha_1/\alpha_2=7/9$, the error introduced by assuming $\alpha_1=\alpha_2$ is approximately 0.5%. Therefore, below we disregard the difference between α_1 and α_2.

The probability amplitude of a single photon at the output of the absorber with a doublet structure is described by Eq. (8) with the transmission function defined in Eq. (14). If we follow the same strategy as in Sec. III and expand the exponent $\exp[-A(\nu)z]$ in a power series, then this probability amplitude is defined by Eq. (11). In the case of a doublet structure, it is difficult to find a general expression for $b_n(t)$ with arbitrary n. We calculated only four terms of this expansion. They are $b_0(t)=\Theta(t)\exp(-\gamma t)$,

$$b_1(t) = -\frac{T\gamma}{2\Delta}\sin(\Delta t) b_0(t), \tag{15}$$

$$b_2(t) = \left(\frac{T\gamma}{4\Delta}\right)^2 \Delta t \, \sin(\Delta t) b_0(t), \tag{16}$$

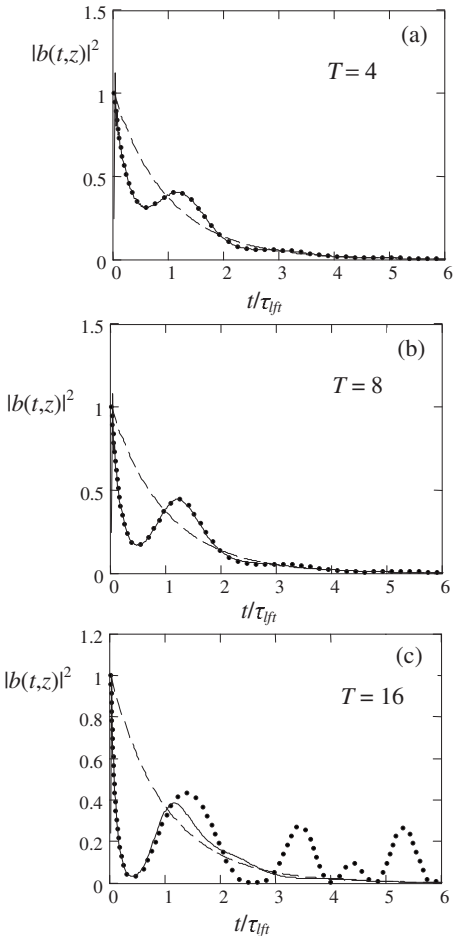

FIG. 2. Time evolution of the photon probability, $|b(t,z)|^2$ at the output of the absorber with effective thickness T. The dashed line shows the photon probability without an absorber. The thin solid line is a result of the numerical integration of Eq. (8). The analytical approximation, Eq. (11), where only four terms of the expansion are taken into account, is shown by dots. Time scale is in units of the lifetime τ_{lft} of the excited nucleus, $\Delta\tau_{\mathrm{lft}}=3.27$.

$$b_3(t) = -\frac{1}{6}\left(\frac{T\gamma}{4\Delta}\right)^3 \{[1+(\Delta t)^2]\sin\Delta t - \Delta t\cos\Delta t\} b_0(t). \tag{17}$$

These terms are sufficient to describe the initial stage of the γ photon decay if the absorber is moderately thick, i.e., if the condition $T\gamma < 4\Delta$ is satisfied. A comparison of the numerically integrated Eq. (8) with the expansion (11), where only the first four terms are taken into account, is shown in Fig. 2. For the plots, we take $\Delta/2\gamma=3.27$ and the time scale is in units of the lifetime of the excited state $\tau_{\mathrm{lft}}=\tau_{\mathrm{ph}}/2$. For optical thicknesses up to $T=8$, our approximation fits excellently the numerical results. In the initial stage, we have destructive interference of the scattered radiation with the incident one because both are in antiphase. Such an interference reflects the absorption of a photon by the nuclei in the absorber. Then, the scattered radiation changes its phase and the interference becomes constructive. The nuclear excitation energy, stored in the absorber, is transformed to the radiation field and the photon probability exceeds its probability without absorber (shown by the dashed line). This process is modulated with frequency Δ. Plots 2(a–c) clearly demonstrate the modulation, which is independent of T if it is not too large. For a larger thickness, $T=16$, our approximation describes well only the destructive stage of the photon interference in the thick absorber.

The approximation, which takes into account a finite number of the expansion terms, cannot correctly describe the time evolution of the photon probability at the output of the absorber for large t. This is because, for example, the third and the fourth terms of the expansion are proportional to t and t^2, respectively. However, our approximation describes well the initial evolution.

V. RESPONSE FUNCTION

In this section, to find the asymptotic behavior of the photon probability for large t, we develop a different approach based on the knowledge of the spectral function for a thick absorber with a doublet structure (transfer function). It allows to calculate the response function of the absorber to a short pulse (impulse response). Then, to calculate the integral in Eq. (8), we apply a convolution theorem.

First, we represent the integrand $F(\nu)\exp(-i\nu t)$ in Eq. (8) as follows:

$$F(\nu)e^{-i\nu t} = B_0(\nu)e^{-A_+(\nu)z}e^{-A_-(\nu)z}e^{-i\nu t}, \tag{18}$$

where z/c is omitted and

$$A_\pm(\nu) = \frac{i\alpha_0/2}{\nu \pm \Delta + i\gamma}. \tag{19}$$

For $B_0(\nu)$, its Fourier counterpart is $b_0(t)$, Eq. (5). For $\exp[-A_\pm(\nu)z]$, the original function is

$$R_\pm(t) = \frac{1}{2\pi}\int_{-\infty}^{+\infty} e^{-i\nu t - A_\pm(\nu)z} d\nu. \tag{20}$$

We calculated this integral. The result is

$$R_\pm(t) = \delta(t) - e^{\pm i\Delta t} b_{\mathrm{sc}}(t), \tag{21}$$

where $\delta(t)$ is the delta function,

$$b_{\mathrm{sc}}(t) = b_0(t)\sqrt{\frac{T\gamma}{4t}} J_1(\sqrt{T\gamma t}), \tag{22}$$

and $J_1(x)$ is the Bessel function of the first order. $R_\pm(t)$ is the response function of a thick absorber with a single resonance to a short deltalike pulse whose spectrum is infinitely wide. Similar expressions have been found in Refs. [24,27,28], where Δ is set equal zero. One can interpret the absorber response, $R_\pm(t)$, as consisting of the prompt radiation (the first term, which is the delta function) and the radiation produced in multiple scattering processes [the second term $\sim b_{\mathrm{sc}}(t)$].

The response function of an absorber with two resonances is

$$R_{ds}(t) = \frac{1}{2\pi}\int_{-\infty}^{+\infty} e^{-i\nu t-[A_+(\nu)+A_-(\nu)]z}d\nu. \quad (23)$$

According to the convolution theorem, it can be expressed as

$$R_{ds}(t) = \int_{-\infty}^{+\infty} R_+(t-\tau)R_-(\tau)d\tau. \quad (24)$$

Integration gives

$$R_{ds}(t) = \delta(t) - 2\cos(\Delta t)b_{sc}(t) + b_{int}(t), \quad (25)$$

where

$$b_{int}(t) = \int_0^t e^{i\Delta(t-2\tau)}b_{sc}(t-\tau)b_{sc}(\tau)d\tau. \quad (26)$$

In Eq. (26), the integral boundaries are defined taking into account the properties of the function $b_{sc}(t)\sim\Theta(t)$.

In case of a doublet structure, the absorber response $R_{ds}(t)$ is the sum of three terms: the prompt radiation, the scattered radiation for each individual resonance of the doublet with its own phase, $\exp(\pm i\Delta t)$, independently, and the radiation, $b_{int}(t)$, produced due to the interference of the radiation scattered on both spectral components, simultaneously.

Applying again the convolution theorem, we obtain for a single photon the following expression at the output of a thick absorber:

$$b(z,t) = \int_{-\infty}^{+\infty} b_0(t-\tau)R_{ds}(\tau)d\tau. \quad (27)$$

This expression can be reduced to

$$b(z,t) = b_0(t)[1 - b_+(t) - b_-(t) + b_{12}(t)], \quad (28)$$

$$b_\pm(t) = \int_0^t e^{\pm i\Delta\tau}f_{sc}(\tau)d\tau, \quad (29)$$

$$b_{12}(t) = \int_0^t dx\int_0^x dy e^{i\Delta(x-2y)}f_{sc}(x-y)f_{sc}(y), \quad (30)$$

where $f_{sc}(t)=b_{sc}(t)/b_0(t)$. The meaning of the terms in Eq. (28) is the same as in the response function, $R_{ds}(t)$, i.e., it is the sum of the prompt radiation, of the scattered radiation formed by the individual resonances, $b_+(t)$ and $b_-(t)$, and the interference term, $b_{12}(t)$.

One can simplify the expression for $b_\pm(t)$ as follows:

$$b_\pm(t) = 1 - e^{\pm i\Delta t}J_0(\sqrt{\beta t}) \pm i\Delta\int_0^t e^{\pm i\Delta\tau}J_0(\sqrt{\beta\tau})d\tau, \quad (31)$$

where $\beta=T\gamma=2\alpha_0 z$. Then, the first three terms inside the square brackets of Eq. (28), $b_{sum}(t)=1-b_+(t)-b_-(t)$, are reduced to

$$b_{sum}(t) = 2\left[\cos(\Delta t)J_0(\sqrt{\beta t}) + \Delta\int_0^t \sin(\Delta\tau)J_0(\sqrt{\beta\tau})d\tau\right] - 1. \quad (32)$$

The first term in the square brackets of Eq. (32) decays to zero as $\sim J_0(\sqrt{\beta t})$. The second term is zero for $t=0$, and it rises oscillatory with time. For $t\to\infty$, it has an asymptote (see Ref. [29])

$$2\Delta\int_0^\infty \sin(\Delta\tau)J_0(\sqrt{\beta\tau})d\tau = 2\cos\left(\frac{\beta}{4\Delta}\right). \quad (33)$$

To estimate the asymptotic behavior of the term $b_{12}(t)$ for $t\to\infty$, we express Eq. (30) as follows:

$$b_{12}(t) = \int_0^t dy e^{-i\Delta y}f_{sc}(y)\int_0^{t-y} d\tau e^{i\Delta\tau}f_{sc}(\tau). \quad (34)$$

Since $f_{sc}(y)\to 0$ for $y\to\infty$, we can approximate

$$\lim_{t\to\infty} b_{12}(t) = \int_0^\infty dy e^{-i\Delta y}f_{sc}(y)\int_0^\infty d\tau e^{i\Delta\tau}f_{sc}(\tau). \quad (35)$$

Then, with the help of the table of integral transforms [29], we find

$$\lim_{t\to\infty} b_{12}(t) = 2\left[1 - \cos\left(\frac{\beta}{4\Delta}\right)\right]. \quad (36)$$

Combining Eqs. (32), (33), and (36), we obtain that

$$\lim_{t\to\infty}[b_{sum}(t) + b_{12}(t)] = 1. \quad (37)$$

Thus, the scattered radiation is delayed and it tends to $b_0(t)$ with time. We have to emphasize that if the coherence time of the source photon, τ_{ph}, and the lifetime of the nuclear coherence in the absorber are equal, the probability amplitude of the radiation field at the output of the absorber is factorized, see Eq. (28), i.e., it can be expressed as the product, $b(z,t)=b_0(t)F(t)$, of the probability amplitude of the input radiation, $b_0(t)$, and some response function of the absorber, $F(t)$. The response function does not depend on τ_{ph} and contains only the parameters Δ and $\beta=2\alpha_0 z$. In the case of a single resonance, the response function is $F(t)=J_0(\sqrt{2\beta t})$. In the case of a doublet, it is $F(t)=1-b_+(t)-b_-(t)+b_{12}(t)$. To simplify this function, we transform the interference term, $b_{12}(t)$, as follows.

With the help of the permutation of integrals and the variable substitution

$$\int_0^t dx\int_0^x dy \to \int_0^t dy\int_y^t dx \to \int_0^t dy\int_0^{t-y} d\tau, \quad (38)$$

the term $b_{12}(t)$ is modified as

$$b_{12}(t) = F_1(t) + F_2(t) + F_3(t) + F_4(t), \quad (39)$$

$$F_1(t) = 1 - \cos(\Delta t)J_0(\sqrt{\beta t}) - 2\Delta\int_0^t \sin(\Delta\tau)J_0(\sqrt{\beta\tau})d\tau, \quad (40)$$

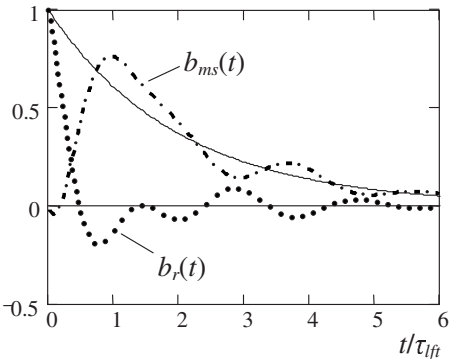

FIG. 3. Time evolution of the probability amplitude $b_r(t)$, dotted line, and $b_{\rm ms}(t)$, dash-dot line. The probability amplitude of the incident photon is shown by the solid line. Time scale is in units of $\tau_{\rm lft}$. Thickness parameter is $T=8$, $\Delta\tau_{\rm lft}=3.27$.

$$F_2(t) = \Delta \int_0^t \sin[\Delta(t-2\tau)] J_0(\sqrt{\beta\tau}) J_0(\sqrt{\beta(t-\tau)}) d\tau, \tag{41}$$

$$F_3(t) = -\int_0^t \cos[\Delta(t-2\tau)] \sqrt{\frac{\beta}{4\tau}} J_1(\sqrt{\beta\tau}) J_0(\sqrt{\beta(t-\tau)}) d\tau, \tag{42}$$

$$F_4(t) = \Delta^2 \int_0^t dy \int_0^{t-y} d\tau \cos[\Delta(y-\tau)] J_0(\sqrt{\beta y}) J_0(\sqrt{\beta\tau}). \tag{43}$$

It can be shown that $F_2(t) \equiv 0$. Then, Eq. (28) is reduced to

$$b(z,t) = b_0(t)[\cos(\Delta t) J_0(\sqrt{\beta t}) + F_3(t) + F_4(t)]. \tag{44}$$

The result can be interpreted as the contribution from "resonant" scattering of the incident radiation on two components of the doublet, modulated with a frequency equal to the doublet splitting, $b_r(t)=b_0(t)\cos(\Delta t)J_0(\sqrt{\beta t})$, plus the interference of these scattering amplitudes, $b_{\rm ms}(t)=b_0(t)[F_3(t)+F_4(t)]$. Their time evolution is shown in Fig. 3. The interference term, $b_{\rm ms}(t)$ (dash-dot line), is delayed and it almost reproduces the probability amplitude of the incident photon for large t (solid line).

Thus, in the case of a doublet structure, the response function is $F(t)=\cos(\Delta t)J_0(\sqrt{\beta t})+F_3(t)+F_4(t)$. If the splitting is zero, $\Delta=0$, then $F_4(t)=0$ and $[\cos(\Delta t)J_0(\sqrt{\beta t})+F_3(t)]|_{\Delta=0}=J_0(\sqrt{2\beta t})$. This result is consistent with the response function of an absorber with a single resonance, $F(t)=J_0(\sqrt{2T\gamma t})$.

VI. GROUP VELOCITY CONCEPT

If the distance between resonances, 2Δ, is much larger than the spectral width of the incident photon, $2\gamma=2/\tau_{\rm ph}$, most of the photon spectrum falls in between the two resonances. This part experiences negligible absorption (resonant loss). Only the long tails of the Lorentzian spectrum of the photon, whose wings drop as $\sim 1/\nu$, are absorbed if $\nu=\pm\Delta$. Meanwhile, the central part of the photon spectrum interacts with the nuclei due to the dispersion $\chi'(\nu)$ (in-phase component of the nucleus response). In the middle of the doublet, this dispersion is normal and one can expect a reduction in the group velocity of the radiation wave packet.

The approximate solution for the single-photon propagation in a dense medium with a transparency window is obtained in Refs. [15,30–32]. It is based on the group velocity concept for the wave packet. Following Refs. [15,30–32], we approximate the transmission function $A(\nu)$ in Eq. (8) by its expansion in a power series near $\nu=0$. It was shown in Refs. [15,30]. that to describe the propagation of the adiabatic part of the pulse (that part whose spectrum is confined inside the transparency window), one can take only four terms of the expansion

$$A(\nu)z \approx \frac{T_{\rm trn}}{2} - i\nu t_d + \frac{\nu^2}{\Delta_{\rm eff}^2} - i\frac{\nu^3}{3\Delta_{\rm dst}^3}, \tag{45}$$

where

$$T_{\rm trn} = \frac{2\alpha_0 z\gamma}{\Delta^2+\gamma^2}, \tag{46}$$

$$t_d = \frac{\alpha_0 z(\Delta^2-\gamma^2)}{(\Delta^2+\gamma^2)^2}, \tag{47}$$

$$\Delta_{\rm eff} = \sqrt{\frac{(\Delta^2+\gamma^2)^3}{\alpha_0 z\gamma(3\Delta^2-\gamma^2)}}, \tag{48}$$

$$\Delta_{\rm dst} = \sqrt[3]{\frac{(\Delta^2+\gamma^2)^4}{3\alpha_0 z[(\Delta^2-\gamma^2)^2-4\Delta^2\gamma^2]}}. \tag{49}$$

The two first terms of the expansion (45) give a reduction in the pulse amplitude and a time delay

$$b_g(z,t) = e^{-T_{\rm trn}/2} b_0(t-t_d). \tag{50}$$

The reduction in the pulse amplitude is defined by the absorption just in the middle of the doublet. The delay of the pulse is caused by the reduction in its group velocity to the value

$$V_g = \left[c^{-1} + \frac{\alpha_0(\Delta^2-\gamma^2)}{(\Delta^2+\gamma^2)^2}\right]^{-1}. \tag{51}$$

The third term of the expansion (45) gives a time broadening of the pulse

$$b_A(z,t) = \frac{\Delta_{\rm eff}}{2\sqrt{\pi}} \int_{-\infty}^{+\infty} b_g(z,\tau) e^{-(\Delta_{\rm eff}/2)^2(t-\tau)^2} d\tau, \tag{52}$$

where the index A in $b_A(z,t)$ means the analytical approximation of Eq. (8). The time broadening of the pulse corresponds to its spectrum narrowing caused by the absorption of the spectral wings of the pulse by the two resonances. For a single-photon wave packet, Eq. (52) is reduced to [31]

$$b_A(z,t) = \phi_+(z,t)\exp[-T_{\rm trn}/2 - \gamma(t-t_d)], \tag{53}$$

where

$$\phi_{\pm}(z,t) = \frac{1}{2} e^{\gamma^2/\Delta_{\text{eff}}^2} \left[1 \pm \text{erf}\left(\frac{\Delta_{\text{eff}}(t-t_d)}{2} \mp \frac{\gamma}{\Delta_{\text{eff}}} \right) \right], \quad (54)$$

erf(x) is the error function. The function $\phi_{-}(z,t)$ will be used below for an incident wave packet with a different shape.

It should be noted that the group delay dispersion, $D_2 = \text{Im}[\partial^2 A(\nu)/\partial \nu^2]|_{\nu=0}$, which is the imaginary part of the third term of the expansion Eq. (45), is zero for a doublet whose spectral components have equal transition probabilities. If the two resonances have different intensities, then $D_2 \neq 0$, and it causes a pulse chirp, accompanied with a pulse broadening in time (see Ref. [32] for details). In this case, the contribution of the group delay dispersion for a doublet structure may be appreciable, as it has been experimentally observed in Refs. [12–14]. Besides, if the carrier frequency of the pulse ω_0 is detuned from the middle of the doublet, ω_m, then the group delay dispersion D_2 also becomes nonzero, even for a doublet with equal strengths for the two resonances. Combining both effects, one can find a particular detuning from the middle of the doublet with nonequal strengths of the absorption lines to compensate fully the group delay dispersion and make it exactly zero. The value of this detuning is found in Ref. [14].

The fourth term of the expansion (45) is responsible for the third order group delay dispersion $D_3 = \text{Im}[\partial^3 A(\nu)/\partial \nu^3]|_{\nu=0}$. Its contribution may result in a distortion of the pulse [30].

In Ref. [30], the competition of the contributions of the third and fourth terms of the expansion (45) in the pulse development in an optically thick medium was studied. It was shown for a Gaussian pulse with a spectral halfwidth Δ_{in} that the spectral halfwidth Δ_{out} of the output pulse (which is still Gaussian if the fourth term of the expansion is not taken into account) is defined by the formula

$$\Delta_{\text{out}} = \frac{\Delta_{\text{in}}}{\sqrt{1 + (\Delta_{\text{in}}/\Delta_{\text{eff}})^2}}. \quad (55)$$

From this expression, it follows that for a thick medium ($T \gg 1$), the pulse spectrum narrows as $\Delta_{\text{out}} \approx \Delta_{\text{eff}} \approx (\Delta^2/\gamma)/\sqrt{3T/2}$ [see Eq. (48)], if $\Delta_{\text{in}} \gg \Delta_{\text{eff}}$ and $\Delta \gg \gamma$. Meanwhile, the contribution of the fourth term becomes effective if the spectrum halfwidth of the modified pulse, Δ_{out}, becomes comparable with or larger than Δ_{dst}. This parameter decreases with thickness T as $\Delta_{\text{dst}} \approx \Delta/\sqrt[3]{3T\gamma/2\Delta}$ [see Eq. (49)]. Therefore, if $\Delta_{\text{in}} \gg \Delta_{\text{eff}}$, the spectrum halfwidth of the pulse decreases faster with thickness increase than the distortion parameter Δ_{dst} and the fourth term of expansion (45) does not contribute to the pulse evolution since $\Delta_{\text{out}} < \Delta_{\text{dst}}$. Formally, this inequality is reduced to $(\Delta/\gamma)^4 < 3T/2$, which holds for $T \to \infty$. Actually, one has to take the experimental values of the parameters of the medium and the input pulse to make a judgment about this competition. For example, in the experiment [14], the doublet splitting is four orders of magnitude larger than the linewidths of the resonances and the spectral width of the pulse is at least ten times smaller than the splitting: $\Delta/\gamma = 10^4$ and $\Delta/\Delta_{\text{in}} = 10$. According to Eq. (55), for these values of the parameters, the spectral width of the output pulse, Δ_{out}, starts narrowing to Δ_{eff} if $T \geq 10^{10}$. Up to this value of thickness, the pulse spectrum does not narrow. Meanwhile, since Δ_{dst} decreases with thickness increase, for $T > 10^7$, we have already satisfied the condition $\Delta_{\text{in}} > \Delta_{\text{dst}}$ of the pulse distortion before its spectrum starts narrowing. This results in the irreversible corruption of the pulse seen as a time broadening and distortion of its central part and an appearance of the wiggles in its trailing edge.

We can show that in our experiment, the third and fourth terms of the expansion (45) almost do not affect the central part of the photon spectrum. For that, we consider the numerical example, given in Sec. IV, where the parameters of the model are typical for our experiment. If in this case we analyze the evolution of the Gaussian pulse whose halfwidth of the spectrum is $\Delta_{\text{in}} = \gamma$ at the input of the medium with the doublet splitting $\Delta \approx 6\gamma$, then $\Delta_{\text{eff}} \approx \Delta_{\text{in}}\sqrt{10^3/T}$, which means that the narrowing of the pulse spectrum starts only when $T \geq 10^3$. According to Eq. (49), the distortion parameter for the given values of the parameters is $\Delta_{\text{dst}} = \Delta_{\text{in}}\sqrt[3]{10^3/T}$. It means that the pulse starts to be distorted also when $T \geq 10^3$. In our experiments, $T < 20$, and hence, the contribution of both terms should be negligible. Meanwhile, the photon wave packet is not Gaussian. It will be shown below that the photon spectrum consists of a Lorentzian (symmetrical part) and an asymmetrical part whose wings drop as $\pm 1/\nu$. The asymmetric part is responsible for the sharp-rising leading edge of the photon wave packet. Photon filtering through the medium with the doublet structure may split the photon wave packets in two components, i.e., the sharp, fast decaying oscillatory component and a smooth, delayed component decaying with the same rate as the input wave packet.

The smoothing of the leading edge of the delayed component is produced by the third term of the expansion (45) [see Eqs. (52) and (53)]. The function $\phi_{+}(z,t)$ in Eq. (53) gives the smoothing of the Heaviside step function in Eq. (50), spreading it around time $t_d + 2\gamma/\Delta_{\text{eff}}^2$. $\phi_{+}(z,t)$ rises from zero to the value $\exp(\gamma^2/\Delta_{\text{eff}}^2)$, which is close to 1 for $\Delta_{\text{eff}} \gg \gamma$. This transient domain is spread in a time interval $\sim 8/\Delta_{\text{eff}}$. The competition of the functions $\phi_{+}(z,t)$ and $\exp[-\gamma(t-t_d)]$ in Eq. (53) shortens this transient domain if T is large enough. As a result, we see a smooth rise of the probability amplitude of the delayed part of the photon followed by a decay.

The time evolution of $b_A(z,t)$, Eq. (53), is shown in Fig. 4(a) for $T=8$ and (b) for $T=80$. The doublet splitting satisfies the condition $\Delta\tau_{\text{lft}} = 3.27$. The estimated value of the transient domain, given only by the contribution of the function $\phi_{+}(z,t)$, is $1.25\tau_{\text{lft}}$ for $T=8$ and it is $4\tau_{\text{lft}}$ for $T=80$. This domain is almost not shortened by the competition of the two functions for $T=8$, but it is shortened to the value $2.6\tau_{\text{lft}}$ for $T=80$.

The function $b_A(z,t)$ gives a nice approximation of the tail of the photon probability amplitude, while its front part is inconsistent with the result of the numerical integration of Eq. (8). This is due to the sharp leading edge of the incident photon, which is defined by the step function $\Theta(t)$. It induces transients dying out quite fast for a thick absorber (see Fig. 4(b), where $T=80$). For a moderately thick absorber [$T=8$, Fig. 4(a)], these transients overlap with the front part of the delayed photon, completely changing the time evolution of the photon probability amplitude. The time delay for $T=80$ is

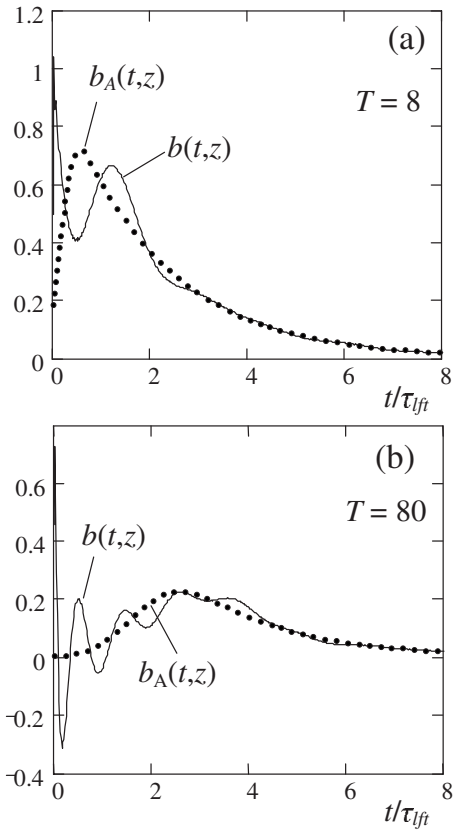

FIG. 4. Time evolution of the analytical approximation of the probability amplitude, $b_A(t)$, the dotted line. The solid line is the result of the numerical calculation of the integral in Eq. (8). The parameters are the same as in Fig. 3. $T=8$ for (a) and $T=80$ for (b).

$t_d=1.744\tau_{\rm lft}$ and for $T=8$ it is $t_d=0.174\tau_{\rm lft}$. In both cases, the leading edge of the delayed part of the probability amplitude of the photon is smooth due to the contribution of the third term of the expansion $A(\nu)z$, Eq. (45). Therefore, instead of $b_g(z,t)$, Eq. (50), we have $b_A(z,t)$, Eq. (53), for the delayed part of the photon.

To describe the transients, which are precursory of the delayed part of the photon, we follow the arguments used in Ref. [31].

We formally represent the Fourier transform of the single-photon field, Eq. (7), as $B_0(\nu)=B_{0s}(\nu)+B_{0a}(\nu)$, where

$$B_{0s}(\nu)=\frac{\gamma}{\nu^2+\gamma^2}, \tag{56}$$

$$B_{0a}(\nu)=\frac{i\nu}{\nu^2+\gamma^2}, \tag{57}$$

are the symmetric and antisymmetric parts, respectively. The first part is an even function whose wings decrease as γ/ν^2. The second part is an odd function whose wings drop as i/ν. Therefore, the antisymmetric part has much longer tails. The time-domain counterparts of these functions are

$$b_{0s}(t)=\frac{1}{2}\exp(-\gamma|t|), \tag{58}$$

$$b_{0a}(t)=\begin{cases}\dfrac{1}{2}\exp(-\gamma t) & \text{if } t>0,\\ 0 & \text{if } t=0,\\ -\dfrac{1}{2}\exp(\gamma t) & \text{if } t<0.\end{cases} \tag{59}$$

The function $b_{0s}(t)$ has no discontinuity, except a discontinuity in its slope. The function $b_{0a}(t)$ is a noncontinuous function. Therefore, the former should not acquire large amplitude transients at the output of a thick absorber, and the latter should have them.

Substituting the amplitudes $b_{0s}(t)$ and $b_{0a}(t)$ into Eq. (27), we obtain the following expressions for these amplitudes at the output of a thick absorber with a doublet structure

$$b_{s,a}(z,t)=\int_{-\infty}^{+\infty} b_{0s,a}(t-\tau)R_{\rm ds}(\tau)d\tau. \tag{60}$$

After some tedious algebra, we obtain

$$b_s(z,t)=\begin{cases}\frac{1}{2}[b(z,t)-b_{\rm tr}(z,t)] & \text{if } t\geq 0,\\ \frac{1}{2}\exp\left(\gamma t-\dfrac{\beta\gamma}{\Delta^2+4\gamma^2}\right) & \text{if } t\leq 0,\end{cases} \tag{61}$$

$$b_a(z,t)=\begin{cases}\frac{1}{2}[b(z,t)+b_{\rm tr}(z,t)] & \text{if } t>0,\\ -\frac{1}{2}\exp\left(\gamma t-\dfrac{\beta\gamma}{\Delta^2+4\gamma^2}\right) & \text{if } t<0,\end{cases} \tag{62}$$

where $b(z,t)$ is defined in Eq. (44) and $b_{\rm tr}(z,t)$ is

$$b_{\rm tr}(z,t)=\sum_{n=1}^{5}\Phi_n(t). \tag{63}$$

The functions $\Phi_i(t)$ are derived in a similar way as the expressions for $b_{\pm}(t)$, see Eq. (31), and for $b_{12}(t)$, see Eq. (39). These functions are

$$\Phi_1(t)=e^{-\gamma t}\cos(\Delta t)J_0(\sqrt{\beta t}), \tag{64}$$

$$\Phi_2(t)=-(\Delta^2+4\gamma^2)e^{\gamma t}[J_c(0)J_c(t)+J_s(0)J_s(t)], \tag{65}$$

$$\Phi_3(t)=e^{-\gamma t}\int_0^t 2\gamma\cos[\Delta(t-2\tau)]J_0(\sqrt{\beta\tau})J_0(\sqrt{\beta(t-\tau)})d\tau, \tag{66}$$

$$\Phi_4(t)=F_3(t)e^{-\gamma t}, \tag{67}$$

$$\Phi_5(t)=-(\Delta^2+4\gamma^2)\int_0^t dy\int_{t-y}^{\infty} d\tau e^{\gamma t-2\gamma(y+\tau)} \times\cos[\Delta(y-\tau)]J_0(\sqrt{\beta y})J_0(\sqrt{\beta\tau}), \tag{68}$$

where

$$J_c(t)=\int_t^{\infty}\cos(\Delta\tau)e^{-2\gamma\tau}J_0(\sqrt{\beta\tau})d\tau, \tag{69}$$

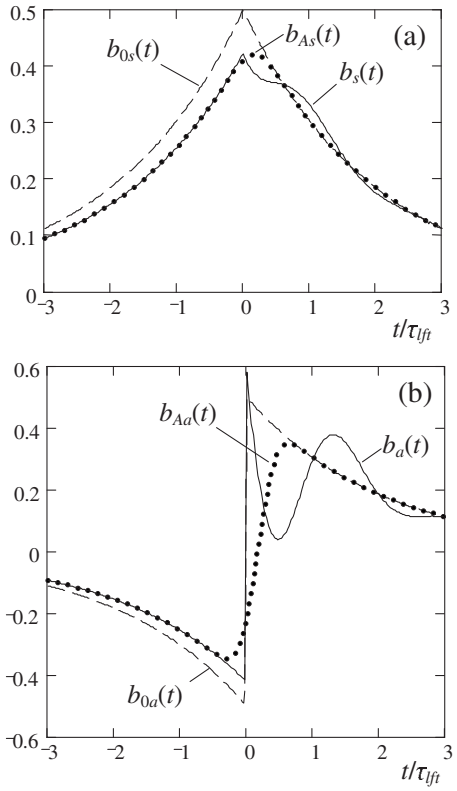

FIG. 5. The time evolution of the symmetric and antisymmetric components of the probability amplitude of the photon at the output of the absorber with effective thickness $T=8$ (solid line). These components at the input are shown by the dashed line. The dotted line shows the approximation obtained with the group velocity approach. The doublet splitting is $\Delta\tau_{\text{lft}}=3.27$.

$$J_s(t) = \int_t^\infty \sin(\Delta\tau) e^{-2\gamma\tau} J_0(\sqrt{\beta\tau}) d\tau. \tag{70}$$

Here, to simplify the expressions, we used the identity

$$J_s^2(0) + J_c^2(0) = \frac{\exp\left(-\dfrac{\beta\gamma}{\Delta^2+4\gamma^2}\right)}{\Delta^2+4\gamma^2}. \tag{71}$$

The group velocity approach, where the transmission function $A(\nu)z$ is approximated by Eq. (45), gives the following expressions for the symmetric and antisymmetric parts of the photon:

$$b_{As}(z,t) = [R_+(z,t) + R_-(z,t)]/2, \tag{72}$$

$$b_{Aa}(z,t) = [R_+(z,t) - R_-(z,t)]/2, \tag{73}$$

where

$$R_\pm(z,t) = \phi_\pm(z,t)\exp[-T_{\text{trn}}/2 \mp \gamma(t-t_d)]. \tag{74}$$

A comparison of this approximation with the exact result, Eqs. (61) and (62), is shown in Fig. 5. The deviation of the approximation from the exact result is caused by discontinuities of the slope of the symmetric component $b_{0s}(t)$ and of the amplitude of the antisymmetric component $b_{0a}(t)$ at $t=0$. The former produces small amplitude transients and the deviation of $b_s(z,t)$ from $b_{As}(z,t)$ is small. The latter produces large amplitude transients and the deviation of $b_a(z,t)$ from $b_{Aa}(z,t)$ is appreciable. Since a single-photon field $b_0(t)$ has a sharp-rising amplitude at $t=0$, which resembles the jump of the amplitude of $b_{0a}(t)$ from $-1/2$ to $+1/2$ at $t=0$, we conclude that just the antisymmetric part, $b_a(z,t)$, gives the dominant contribution to the transients.

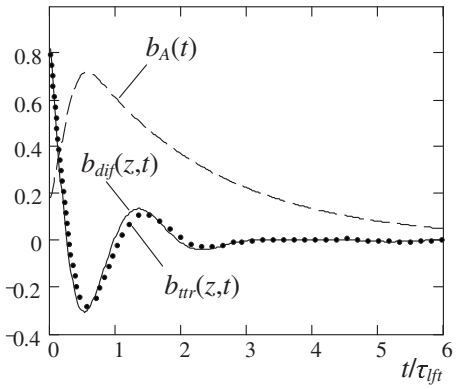

FIG. 6. The time evolution of the true transients $b_{\text{ttr}}(z,t)$ (dots) and of the difference $b_{\text{dif}}(z,t)=b(z,t)-b_A(t,z)$ (solid line). The time evolution of the delayed component of the photon, $b_A(z,t)$, is shown for comparison. The parameters are the same as in Fig. 5.

If we take the difference between the antisymmetric and symmetric components, we can expect that for $t \geq 0$, this difference is a good approximation for the transients following the sharp leading edge of the probability amplitude of a single-photon

$$b_a(z,t) - b_s(z,t) = b_{\text{tr}}(z,t). \tag{75}$$

Meanwhile, according to the group velocity approach, the difference between the slow components of the antisymmetric and symmetric parts of the photon is

$$b_{Aa}(z,t) - b_{As}(z,t) = -R_-(z,t). \tag{76}$$

Therefore, the true transients are described by the difference of Eqs. (75) and (76)

$$b_{\text{ttr}}(z,t) = b_{\text{tr}} + R_-(z,t). \tag{77}$$

Combining these relations, we approximate the probability amplitude of the photon at the output of a thick absorber as

$$b(z,t) \approx b_A(z,t) + b_{\text{ttr}}(z,t). \tag{78}$$

Here, the first term, $b_A(z,t)$, describes the delayed part of the photon, and the second term, $b_{\text{ttr}}(z,t)$, describes the transients induced by the sharp leading edge of the photon. Fig. 6 shows a comparison of the exact difference of $b(z,t)$ and $b_A(z,t)$, which is $b_{\text{dif}}(z,t)=b(z,t)-b_A(z,t)$, (solid line) with our approximation, Eq. (77), $b_{\text{ttr}}(z,t)$ (dotted line). Both plots almost coincide in a wide range of the time scale. The transients decay fast, experiencing two wiggles, i.e., one dip with a negative amplitude and one bump with a positive amplitude. The time dependence of the delayed part of the photon (dashed line) is shown for comparison. It has one bump coinciding with the negative dip of the transients. Therefore, we have destructive interference of the delayed part of the

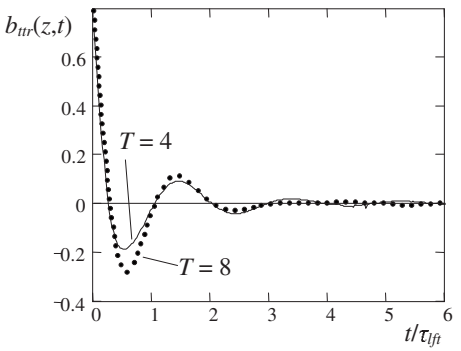

FIG. 7. Time evolution of the transients $b_{\mathrm{ttr}}(z,t)$ for $T=4$ (solid line) and $T=8$ (dots). The doublet splitting is $\Delta\tau_{\mathrm{lft}}=3.27$.

photon with transients. Then, when the positive bump appears, we have a constructive interference of the delayed part and the transients. The frequency of the transients is defined by the doublet splitting Δ. Therefore, for moderately thick samples, $T\sim 8$, quantum beats with frequency Δ result in a delay of the photon for a time $\sim\tau_{\mathrm{lft}}$. Figure 7 shows the transients $b_{\mathrm{ttr}}(z,t)$ for $T=4$ (solid line) and for $T=8$ (dots). It is clearly seen, that for samples with moderate thickness, the frequency of transients is mostly defined by Δ.

VII. EXPERIMENT

A Mössbauer experiment is performed by measuring the transmission of recoilless γ radiation through a resonant absorber whose resonance may be shifted due to a small relative velocity between the source and absorber. We make use of the most popular Mössbauer isotope, ^{57}Fe, incorporated into a solid as an absorber. The appropriate γ photon source for ^{57}Fe consists of ^{57}Co nuclei, which decay via a two-photon cascade. The source nucleus decays by electron capture to ^{57m}Fe with nuclear spin $I=5/2$, which decays in turn by emission of a 122 keV photon followed by a 14.4 keV photon (competing with internal conversion) to the ground state with nuclear spin $I=1/2$. The decay scheme of ^{57}Co is

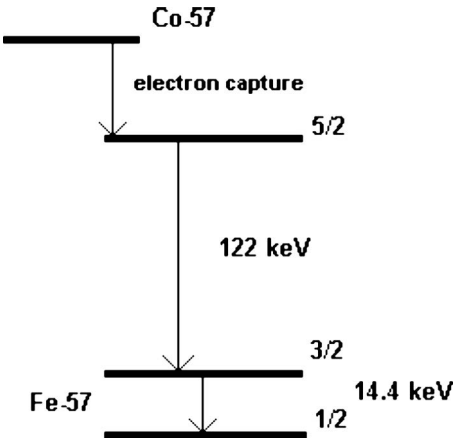

FIG. 8. Decay scheme of the source nucleus ^{57}Co.

shown in Fig. 8. For ^{57}Co in Rh matrix at room temperature, the 14.4 keV photon is the one that is emitted without recoil about 75% of the time. We measure the transmission of the 14.4 keV photon through a resonant absorber. The transmitted photons are counted in delayed coincidence with 122 keV photons. The time-domain spectrum of the transmitted radiation gives information on the temporal aspects of the emission and absorption processes involved, with well-defined initial conditions. In this scheme, the formation of the 14.4 keV nuclear state with spin $I=3/2$ in the source is announced by the detection of a 122 keV photon emitted in a two-photon cascade of the decay of ^{57}Co.

We make use of the conventional experimental setup for time-differential Mössbauer spectroscopy. The schematic arrangement of the source, absorber, detectors, and electronics is shown in Fig. 9. The source, ^{57}Co:Rh, is mounted on the holder of the Mössbauer drive, which is used to Doppler shift the frequency of the radiation of the source. The 122 keV γ photons are detected by a NaI(Tl) scintillator 25 mm in diameter and 15 mm in length, coupled to an RCA 8575 photomultiplier. This detector is mounted about 50 mm away from the source in a direction making an angle of 60° with

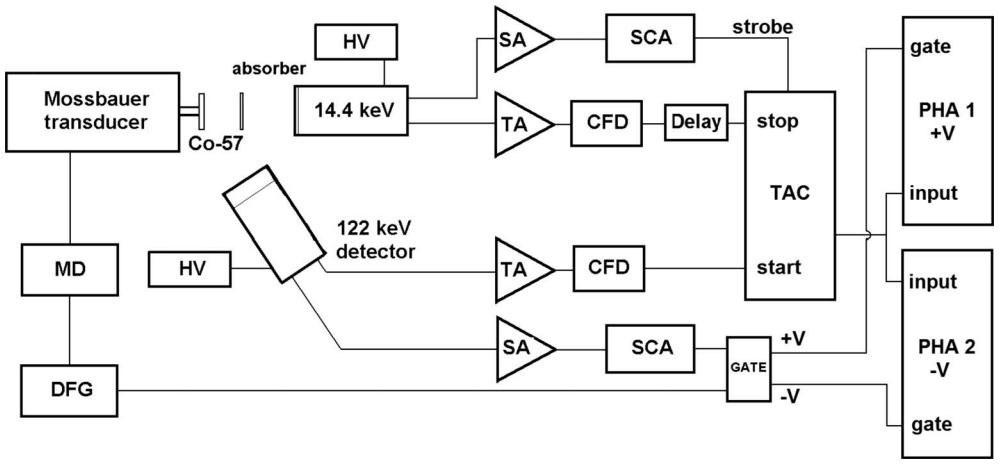

FIG. 9. Simplified scheme of the experimental setup. TAC is a time-to-amplitude converter. PHA is a pulse-height analyzer. TA is a timing amplifier. SA is a spectroscopy amplifier. SCA is a single-channel analyzer. DFG-MD is the Mössbauer driving unit and function generator. HV is a high-voltage supply.

the forward direction, defined by the line from the source to the 14.4 keV detector. The lower-energy radiation (14.4 keV) is filtered out with a 0.1 mm copper foil placed in front of the 122 keV detector. The output from the fast dynode of the photomultiplier is amplified with a timing filter amplifier (2111, Canberra) and triggered by a constant fraction discriminator (2121, Canberra). This timing pulse was employed to produce a start signal for the time-to-amplitude converter (TAC/SCA 2145, Canberra). A second detector with a NaI(Tl) scintillator, 25 mm in diameter and 0.1 mm thick, is served as a detector for the 14.4 keV γ photons. The fast pulse is amplified by the Model 2111 timing filter amplifier and triggered by the Model 2121 constant fraction discriminator to derive a time-pickoff signal, and then it is fed through an adjustable delay line into the stop input of the TAC. The slow pulses from the 14.4 keV detector are amplified with the spectroscopy amplifier. The timing single-channel analyzer (AMP&TSCA, model 290A, Ortec) is utilized to select the 14.4 keV γ photons. These signals are used as strobe signals to generate the TAC output pulses corresponding to the time intervals between the 122 keV and successive 14.4 keV γ quanta. To avoid the undesirable effect of scattered x-rays and Compton radiation [33], the detectors are shielded with lead plates. The output of the TAC consists of pulses of various heights corresponding to different time intervals between the 122 and 14.4 keV γ rays. These pulses are analyzed by two CMCA-550 data acquisition cards (Wissel) in pulse-height mode (PHA). The selection of the card to store the signal is gated by the incoming signal from the Mössbauer driver function generator, which defines the frequency of the radiation of the source. When the source is driven with a velocity corresponding to the central frequency of the sample doublet, the time-domain spectrum is stored in the memory of the first card. The second acquisition card is used to store the time spectrum when the frequency of the radiation of the source is far away from the doublet center. The spectrometer (TAC and data acquisition card operating in PHA mode) is calibrated with a Tektronix RM 181 time marker and a Tektronix TDS 2022 oscilloscope.

A typical time spectrum of the decay of 14.4 keV state (with no absorber) is shown in Fig. 10. A time resolution of 9.1(5) nsec is obtained by least squares fitting the lifetime spectra with the convolution of the theoretical decay curve and a Gaussian distribution originating from the time resolution function of the experimental setup (see, for example, Ref. [34] for details). The curve obtained for a single line source ^{57}Co shows the single exponential decay with a mean lifetime $\tau_{\mathrm{lft}}=1/2\gamma$ of 140.(9) nsec, in good agreement with the mean lifetime and the natural linewidth data for the 14.4 keV state of ^{57}Fe. Here, for simplicity, we define a parameter $\Gamma_0=2\hbar\gamma$, which is reciprocal to the inverse value of the lifetime of the 14.4 keV state and the full width at half-maximum of the 14.4 keV emission line. We assume that it is defined only by natural broadening caused by radiative decay and internal conversion. The contribution of the latter is 93% [17].

The time-domain experiments with absorbers obviously placed between the source and the detector, were performed for absorbers with different splittings of the doublet structure and different thickness. Among them are samples with natural ^{57}Fe abundance [$FeTiO_3$, $FeC_2O_4\cdot 2H_2O$, and $Fe_2(SO_4)_3\cdot xH_2O$], which are commercial products from Alfa Aesar. The ^{57}Fe-enriched ferric sulfate absorbers were home made by the method described in Ref. [35].

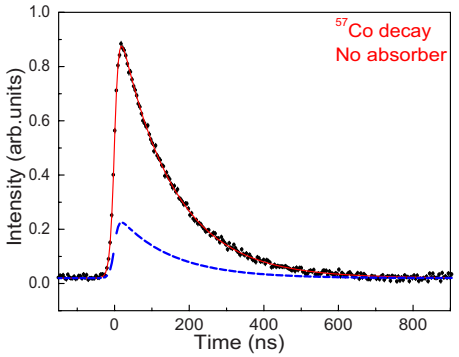

FIG. 10. (Color online) The lifetime curve measured for the 14.4 keV radiation of ^{57}Co (dots). The solid line is the best fit using exponential decay with 141 nsec mean lifetime. The dashed line corresponds to the radiation with recoil. It is described by the convolution of the theoretical curve, Eq. (81), with a Gaussian distribution accounting for the experimental time resolution σ =9.1(5) nsec.

To determine the absorber parameters, such as doublet splitting, effective thickness, and linewidth, we measured their frequency-domain spectra. Mössbauer spectra of the samples are shown in Fig. 11. To analyze in a consistent manner the transmission profiles for the last three samples,

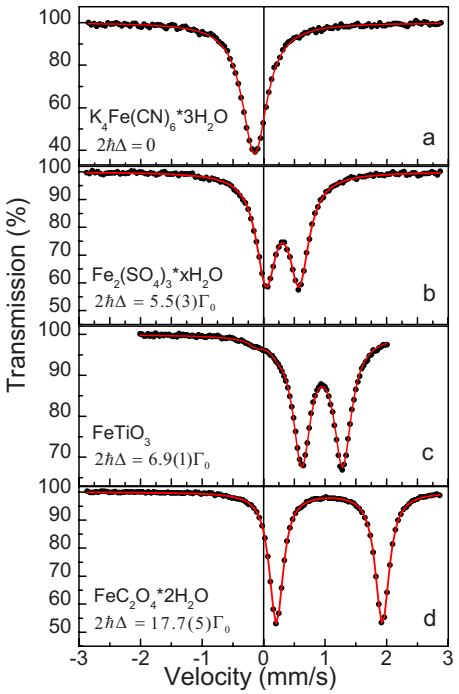

FIG. 11. (Color online) Mössbauer transmission spectra of $K_4Fe(CN)_6\cdot 2H_2O$ (a), $Fe_2(SO_4)_3\cdot xH_2O$ (b), $FeTiO_3$ (c), and $FeC_2O_4\cdot 2H_2O$ (d) measured with ^{57}Co:Rh source (dots). Γ_0 =0.097 mm/sec is the natural linewidth of the 14.4 keV energy level of ^{57}Fe isotope. The solid curves are theoretical fits to Eq. (79).

we have to accept that the profiles consist of quadrupole-split doublets. Because of the isomer shift, the central frequencies of these doublets are different from the position of the single line 14.4 keV of the source ^{57}Co:Rh. This shift is 0.31(1) mm/sec for ferric sulfate (b), 0.95(1) mm/sec for ilmenite (c), and 1.07(1) mm/sec for iron oxalate dihydrate (d). The separation between the absorption peaks $2\hbar\Delta$ for these samples is $5.5(3)\Gamma_0$ (b), $6.9(1)\Gamma_0$ (c), and $17.7(5)\Gamma_0$ (d), where $\Gamma_0 = 0.097$ mm/sec. Here, Γ_0 is defined in units of the small relative velocity v between the source and the absorber, which produces a shift $E_0 v/c$, where E_0 is photon energy and c is the speed of light in vacuum. The Mössbauer spectra of the absorbers were fitted using the transmission integral, $\varepsilon(v)$ [36],

$$\varepsilon(v) = \frac{\Gamma_0}{2\pi}\int_{-\infty}^{+\infty} \frac{1 - f_S + f_S e^{-\varphi_+(E)-\varphi_-(E)}}{\left(E + \frac{v}{c}E_0\right)^2 + \frac{\Gamma_0^2}{4}} dE, \tag{79}$$

$$\varphi_\pm(E) = \frac{T_A}{2} \frac{\frac{\Gamma_A^2}{4}}{(E - E_\delta \pm \hbar\Delta)^2 + \frac{\Gamma_A^2}{4}}, \tag{80}$$

where T_A is the effective thickness of the absorber, Γ_A is the full width of the absorption line of ^{57}Fe in the absorber (in energy units), which includes also other broadening mechanisms on top of the natural broadening, E_δ is the energy shift in the center of the doublet, and f_S is the recoilless fraction of the source radiation. This fitting allows to derive the parameters E_δ, Γ_A, and $T_A = n\sigma_0 f_A$ of the absorber, where n is the number of ^{57}Fe nuclei in the absorber per unit area, σ_0 is the maximum resonant absorption cross section for the 14.4 keV transition, and f_A is the recoilless fraction of the γ ray absorption in the absorber. We found that the linewidths of the selected absorbers was close to the natural one. Meanwhile, the linewidth of ferric sulfate is almost 25% broader than the Mössbauer linewidth of the ilmenite and iron oxalate dihydrate.

To derive the value of the recoilless fraction, f_S, for the source, we use two methods. One is the "black" absorber method [37], where the photon count rates with and without absorber, in resonance and far from resonance are compared. The other method consists of time-domain experiments where we measure the delayed-coincidence counts when a single line filter $[K_4Fe(CN)_6 \cdot 3H_2O]$ of known effective thickness is placed before the detector, what is described in Ref. [19]. A weighted average of both measurements yields the f_S value of 0.75(9), which is in good agreement with that reported in previous publications (see, for example, Ref. [38]).

To simplify the analysis of the time-domain experimental data for samples with a different separation between the lines in the doublet, we selected the samples with almost the same effective Mössbauer thickness, $T_A \approx 5.7$. The results of the delayed-coincidence measurements of the 14.4 keV photon transmission through these samples are shown in Fig. 12. Another set of experimental data, when the splitting is constant, $2\hbar\Delta = 5.5(3)\Gamma_0$, and the effective thickness T_A varies, is shown in Fig. 13. In both figures, the background due to accidental coincidences and the fraction of radiation with recoil, which is nonresonant for the absorber, are subtracted. The background is defined from the counting rate at times preceding the fast front of the incident pulses. A contribution from the radiation with recoil, n_{nr}, is shown in Fig. 10 by the dotted line. Its theoretical time dependence is

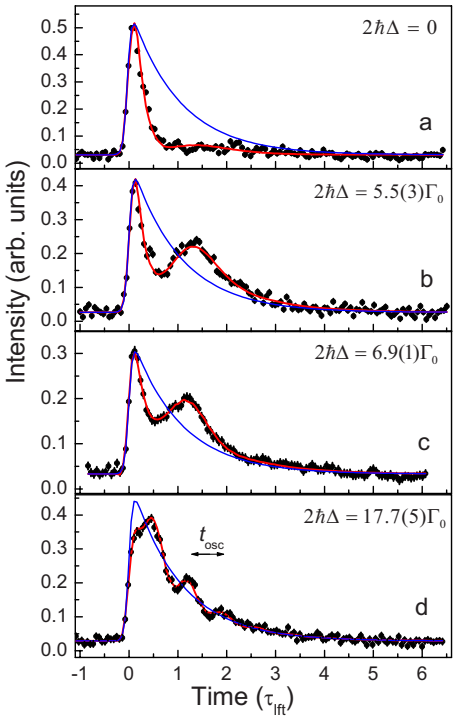

FIG. 12. (Color online) The delayed-coincidence spectra for samples with various doublet splittings and the same effective thickness $T_A \approx 5.7$ (dots). The thick solid line (in red) shows the theoretical fit. The thin solid line (in blue) shows the lifetime curve, measured without absorber. It is scaled to take into account nonresonant losses in the absorber. In plot (d), the arrows indicate a period, t_{osc}, of oscillations with frequency 2Δ. The time scale is in units of the lifetime τ_{lft} of the 14.4 keV state.

$$n_{nr} = \Theta(t)(1 - f_S)e^{-t/\tau_{lft}}. \tag{81}$$

In Fig. 10, this function is convoluted with a Gaussian distribution accounting for the experimental time resolution. The radiation with recoil passes through the absorber with no change since it is not resonant for ^{57}Fe nuclei. Therefore, this radiation carries no information about the absorber and it can be safely removed from the data.

We fitted the raw experimental data, with the background subtracted, to the expression, which is derived as follows. We calculate the transmitted radiation according to the formula

$$n(t) = n_{nr} + f_S n_r, \tag{82}$$

where n_r is the resonant fraction of the radiation, transmitted through the absorber. This fraction is described by

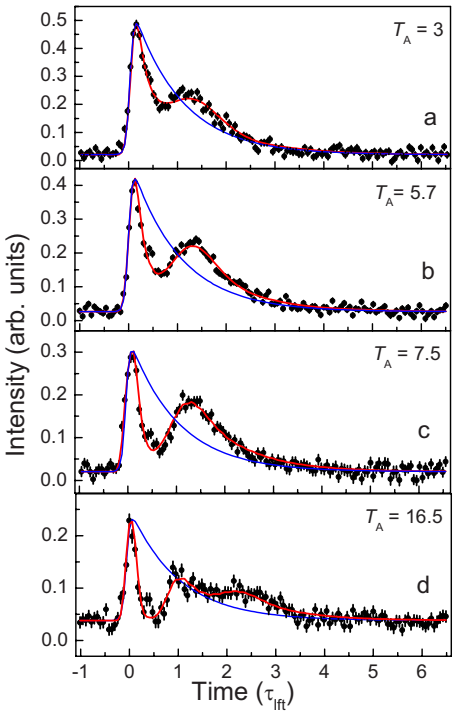

FIG. 13. (Color online) The delayed-coincidence spectra for the $Fe_2(SO_4)_3 \cdot xH_2O$ samples with different thickness (dots). The splitting is $2\hbar\Delta = 5.5(3)\Gamma_0$. The other notations are the same as in Fig. 12.

$$n_r = \left| \frac{\gamma}{\pi} \int_{-\infty}^{+\infty} \frac{\exp[-i\nu t - i\psi_+(\nu) - i\psi_-(\nu)]d\nu}{\nu + i\gamma} \right|^2, \quad (83)$$

where

$$\psi_\pm(\nu) = \frac{T_A}{4} \frac{\frac{\Gamma_A}{2\hbar}}{\nu \pm \Delta + i\frac{\Gamma_A}{2\hbar}}. \quad (84)$$

We convolute $n(t)$ with the Gaussian function

$$n_{\exp}(t) = \frac{1}{\sqrt{2\pi}\sigma} \int_{-\infty}^{+\infty} n(u) e^{-(t-u)^2/2\sigma^2} du, \quad (85)$$

where σ is the standard deviation of the prompt coincidence distribution, taken from the lifetime measurements. When the best fit of the experimental data is obtained, we subtract the fraction of radiation with recoil. Therefore, the plots in Figs. 12 and 13 contain information only about the propagation of the resonant radiation through the absorber without nonresonant losses. It is remarkable that all plots in Figs. 12 and 13, except in Fig. 13(d), are perfectly described by the approximation, given in Sec. IV, which takes into account only four terms of the expansion, Eq. (11).

VIII. DISCUSSION

As it is expected from the theoretical analysis, the experimentally observed time evolution of the γ photon, propagating through an absorber with two absorption lines, shows the so-called speed-up effect of γ decay and a revival of the radiation field, the so-called dynamical beats, which follow the fast decay.

Three stages of the photon evolution are clearly seen from our data. In the first stage, close to $t=0$, the absorber transmits almost all incident γ radiation because the absorption by the resonant medium cannot take place instantaneously. This behavior is very similar to the Sommerfeld-Brillouin prompt pulse known in optics [39]. In the second stage, the γ photon experiences destructive interference with the scattered radiation because both are in antiphase. During this period of time, the radiation is stored in the excited state nuclei. We can consider such an excitation of the nuclei, participating in the scattering process, as the formation of a subradiant (antiphase) state. In the third stage, the scattered radiation changes its phase due to the amplitude oscillation with frequency Δ. The interference with the incoming radiation becomes constructive and the stored energy is emitted as a bump whose amplitude exceeds the amplitude of the radiation with no absorber. So, we have a superradiant state.

The bump in the photon probability is clearly seen in the experimental time-spectra. According to our theoretical analysis and experimental spectra, the phase of the collectively scattered radiation is modulated with the frequency of the doublet splitting Δ. For the absorber with no splitting [see Fig. 12(a)], there is no bump because the doublet splitting frequency is zero and the expected moment of the bump revival is pushed to infinity. An increase in the doublet splitting leads to the appearance of at least one well-defined bump. In Fig. 12, where the effective thickness is kept constant $T_A \approx 5.7$, we see that the bump position depends on $2\hbar\Delta$. With a splitting increase from $5.5(3)\Gamma_0$ (b) to $6.9(1)\Gamma_0$ (c) and then to $17.7\Gamma_0$ (d), the oscillation period shortens. For a large splitting, $2\hbar\Delta = 17.7\Gamma_0$, several bumps are observed since the period of the phase oscillations becomes shorter than the lifetime, τ_{lft}. The observed time separation between successive bumps, $t_{\text{osc}} \sim 100$ nsec, indicated in Fig. 12(d) by arrows, is in good agreement with the doublet splitting $\Delta = 0.86(1)$ mm/sec, which corresponds to 10.0(1) MHz. We should mention that in Fig. 12(d), the first bump overlaps with the speedup, changing appreciably the initial decay picture. The short prompt at $t=0$ is not clearly seen as a sharp peak because of the convolution with a relatively broad Gaussian function.

The delayed-coincidence spectra for $Fe_2(SO_4)_3 \cdot xH_2O$ samples with the same splitting $2\hbar\Delta = 5.5(3)\Gamma_0$, but a different thickness are shown in Fig. 13. The thicker the sample is, the faster the speed-up effect is. Meanwhile, the position of the bump is nearly the same for the samples with moderate thickness, Figs. 13(a)–13(c). For the sample with large thickness, Fig. 13(d), the bump amplitude reduces close to the level defined by the photon probability with no absorber. Thus, the amplitude of the bump grows with thickness increase from $T_A = 3$ to $T_A = 5.7$ and $T_A = 7.5$, taking its maximum for the last two values, and then decreases when $T_A = 16.5$. The position of the bump also changes, moving slightly to longer times and then coming back with thickness increase.

We conclude that there is a competition between the thickness effect due to multiple scattering and the phase re-

versal of the scattered radiation due to oscillations with the doublet splitting. Multiple scattering is an irreversible process because the phase of the radiation changes at each scattering event and when we have many scattering (rescattering) events the radiation field consists of many components with different phases. Their destructive interference results in radiation damping, seen as speedup. The modulation of the phase of the scattered radiation due to the doublet splitting is reversible (dynamical) process, which is repeated with a well-defined period. If the absorber is moderately thick, the modulation can compete with the thickness effect and restore the photon probability. Otherwise, even the phase reversal of the scattered radiation as a whole does not help to restore the radiation field.

We estimated the group velocity V_g of the propagation of the pulsed radiation in an $FeTiO_3$ sample with effective thickness $T_A \approx 5.7$ and physical thickness $z=107$ micron [Fig. 12(c)]. According to Eq. (51), we obtain $V_g = 6.75$ km/sec, which is $4.44 \cdot 10^4$ times smaller than the speed of light in vacuum. Meanwhile, the delay of photon in our samples is mostly defined by the transition of the radiation-absorber compound system from a subradiant to a superradiant state due to the dynamics of the doublet coherence of the nuclei. The actual delay of the photon for the $FeTiO_3$ sample with effective thickness $T_A \approx 5.7$ is 10.3 times longer. If we define the effective group velocity, V_{eff}, of the pulsed radiation as the physical length of the sample divided by the delay time (position of the bump from $t=0$), then $V_{\text{eff}}=660$ m/sec, which is $4.5 \cdot 10^5$ times smaller than the speed of light in vacuum.

Concluding this section, we have to clarify that the slow photon is described in a group velocity concept by the approximate equation (50), where the delay time t_d of the photon in an absorber of physical thickness z is related to the group velocity V_g, Eq. (51), as $V_g t_d = z$. The delay time t_d is short for moderately thick samples. For example, for the sample with thickness $T_A \approx 5.7$ and splitting $2\hbar\Delta = 6.9\Gamma_0$, we have $t_d = 15.8$ nsec. In the idealized equation (50), where only the group velocity change is taken into account, the probability amplitude of the photon has a sharp-rising leading edge at $t=t_d$ and an exponentially decaying tail. Actually, due to the frequency filtering effect (see Ref. [31] for details), the probability amplitude of the slow photon part is described by Eq. (53). As a result, the leading edge of the probability amplitude of a slow photon is smoothened and spread in time, such that its maximum can take place at a time before the bump or after it, depending on the effective thickness (see, for example, Fig. 4). For the sample, discussed above, this maximum takes place at the first minimum before the bump of the photon probability, calculated without approximations. This difference between the predictions of the group velocity concept and the actual time behavior of the radiation field in the absorber is due to the stepwise rise of the photon probability at time $t=0$ (see discussion in Sec. VI).

IX. CONCLUSION

We found theoretically and experimentally an appreciable delay of a γ photon propagating in an absorber with two resonances. This delay is comparable with the lifetime of the excited state nuclei in the absorber. Storage and retrieval of γ radiation in the absorber is explained by the transition from a subradiant to a superradiant state of the radiation-absorber combined system. Initially, the radiation field, scattered by the absorber is in antiphase with the incoming radiation field. This results in destructive interference of both fields, seen as an essential drop in intensity of the output radiation. Then, due to the nuclear coherence oscillation with a frequency corresponding to the doublet splitting, the scattered radiation changes its phase such that both the incoming and scattered radiation become in-phase and, hence, interfere constructively. This is seen as a bump in the probability of the output radiation, which exceeds the probability of the radiation with no absorber.

To our knowledge, the interaction of a single photon with a resonant medium has not yet been experimentally studied in the optical domain. Instead, faint laser pulses or a radiation field, which is produced in parametric down conversion (this field contains not only photon pairs, but also four, eight, etc. photons with much smaller probability) are used in optical experiments to simulate single-photon sources. Until now, Mössabuer spectroscopy is probably a unique tool to study the interaction of a single photon with two- and three-level particles. It has two major advantages. The first is the high efficiency of γ detectors since the energy of recoilless γ photons is ranged between 10 and 100 keV. The second advantage is the long coherence time of the source photons, long enough to use simple electronics operating at frequencies not higher than 100 MHz or in a time scale not shorter than 1–10 nsec.

The findings of our paper may be applied in the optical domain to filter single photons through a resonant medium of moderate thickness. This filtering separates in time and space the sharp (broadband) leading edge of the photon wave packet, which produces precursors, from the smooth delayed part of the photon. As has been shown in Ref. [31], the smooth part has a much higher probability to interact with a resonant medium, which is proposed to serve as an optical memory.

ACKNOWLEDGMENTS

This work was supported by the FWO Vlaanderen, National Science Foundation (USA), Russian Foundation for Basic Research (Grant No. 09-02-00206-a), Program of Presidium of RAS "Quantum physics of condensed matter," and Grant of Federal Agency on Education, Russia (Grant No. NK—02.740.11.0428).

[1] Michael A. Nielsen and Isaac L. Chuang, *Quantum Computation and Quantum Information* (Cambridge University Press, Cambridge, England, 2000); N. Gisin, G. Ribordy, W. Tittel, and H. Zbinden, Rev. Mod. Phys. **74**, 145 (2002); P. Kok, W. J. Munro, K. Nemoto, T. C. Ralph, J. P. Dowling, and G. J. Milburn, *ibid.* **79**, 135 (2007).
[2] G. V. Smirnov, Hyperfine Interact. **123-124**, 31 (1999).
[3] G. T. Trammell, *Proceedings of the International Atomic Energy Agency Symposium on Chemical Effects of Nuclear Transformations*, Prague, 1960 (IAEA, Vienna, 1961), Vol. 1, p. 75.
[4] Yu. Kagan and A. M. Afanas'ev, *Proceedings of the International Atomic Energy Agency Symposium on Mössbauer Spectroscopy and its Application* (IAEA, Vienna, 1972), p. 143.
[5] J. I. Cirac, P. Zoller, H. J. Kimble, and H. Mabuchi, Phys. Rev. Lett. **78**, 3221 (1997).
[6] S. E. Harris, Phys. Today **50**(7), 36 (1997).
[7] M. Fleischhauer, A. Imamoglu, and J. P. Marangos, Rev. Mod. Phys. **77**, 633 (2005).
[8] C. Liu, Z. Dutton, C. H. Behroozi, and L. V. Hau, Nature (London) **409**, 490 (2001).
[9] D. Phillips, A. Fleischhauer, A. Mair, R. Walsworth, and M. D. Lukin, Phys. Rev. Lett. **86**, 783 (2001).
[10] K. Akiba, K. Kashiwagi, T. Yonehara, and M. Kozuma, Phys. Rev. A **76**, 023812 (2007).
[11] H. Tanaka, H. Niwa, K. Hayami, S. Furue, K. Nakayama, T. Kohmoto, M. M. Kunitomo, and Y. Fukuda, Phys. Rev. A **68**, 053801 (2003).
[12] R. M. Camacho, M. V. Pack, and J. C. Howell, Phys. Rev. A **73**, 063812 (2006).
[13] R. M. Camacho, C. J. Broadbent, I. Ali-Khan, and J. C. Howell, Phys. Rev. Lett. **98**, 043902 (2007).
[14] R. M. Camacho, M. V. Pack, J. C. Howell, A. Schweinsberg, and R. W. Boyd, Phys. Rev. Lett. **98**, 153601 (2007).
[15] R. N. Shakhmuratov and J. Odeurs, Phys. Rev. A **77**, 033854 (2008).
[16] M. O. Scully and M. S. Zubairy, *Quantum Optics* (Cambridge University Press, Cambridge, England, 1997), p. 208.
[17] F. J. Lynch, R. E. Holland, and M. Hamermesh, Phys. Rev. **120**, 513 (1960).
[18] R. E. Holland, F. J. Lynch, G. J. Perlow, and S. S. Hanna, Phys. Rev. Lett. **4**, 181 (1960).
[19] N. Hayashi, T. Kinoshita, I. Sakamoto, and B. Furubayashi, Nucl. Instrum. Methods **134**, 317 (1976).
[20] E. I. Vapirev, P. S. Kamenov, D. L. Balabansky, S. I. Ormadjiev, and K. Yanakiev, J. Phys. (Paris) **44**, 675 (1983).
[21] M. Haas, V. Hizhnyakov, E. Realo, and J. Jögi, Phys. Status Solidi B **149**, 283 (1988).
[22] W. C. McDermott III and G. R. Hoy,Hyperfine Interact. **107**, 81 (1997).
[23] S. M. Harris, Phys. Rev. **124**, 1178 (1961).
[24] M. D. Crisp, Phys. Rev. A **1**, 1604 (1970).
[25] U. van Bürck, Hyperfine Interact. **123-124**, 483 (1999).
[26] G. Hoy, J. Phys.: Condens. Matter **9**, 8749 (1997).
[27] D. C. Burnham and R. Y. Chao, Phys. Rev. **188**, 667 (1969).
[28] Yu. Kagan, A. M. Afanas'ev, and V. G. Kohn, J. Phys. C **12**, 615 (1979).
[29] *Tables of Integral Transforms*, edited by A. Erdélyi (McGraw-Hill, New York, 1954).
[30] R. N. Shakhmuratov and J. Odeurs, Phys. Rev. A **71**, 013819 (2005).
[31] R. N. Shakhmuratov, J. Odeurs, and P. Mandel, Phys. Rev. A **75**, 013808 (2007).
[32] R. N. Shakhmuratov and J. Odeurs, Phys. Rev. A **78**, 063836 (2008).
[33] W. C. McDermott, D. E. Johnson, and G. R. Hoy, Hyperfine Interact. **92**, 1077 (1994).
[34] J. C. Dehaes, Nucl. Instrum. Methods **120**, 301 (1974).
[35] A. R. Champion, R. W. Vaughan, and H. G. Drickamer, J. Chem. Phys. **47**, 2583 (1967).
[36] S. Margulies and J. R. Ehrman, Nucl. Instrum. Methods **12**, 131 (1961).
[37] R. M. Housley, N. E. Erickson, and J. G. Dash, Nucl. Instrum. Methods **27**, 29 (1964).
[38] J. Ball and S. J. Lyle, Nucl. Instrum. Methods **163**, 177 (1979).
[39] L. Brillouin, *Wave Propagation and Group Velocity* (Academic Press, New York, 1960).